

**Proceedings of the First
Polish-Korean Seminar
on Structural and Physical Properties
of Magnetic Materials**

**August 24~30, 1995
CheongJu, Korea**

**Sponsored by
Polish Academy of Sciences
and
Korea Science and Engineering Foundation**

Mesoscopic aspects of the spin glass behavior

D. Kaptás⁺, T. Kemény⁺, L.F. Kiss⁺, J. Balogh⁺ and I. Vincze^{+,**}

⁺Research Institute for Solid State Physics, H-1525 Budapest, P.O.B. 49, Hungary

^{**}Solid State Physics Department, Eötvös University, Budapest, Hungary

Abstract-An overview will be given on recent composition, temperature and external magnetic field dependence studies of the magnetic properties of melt-quenched amorphous $\text{Fe}_{100-x}\text{Zr}_x$ ($7 \leq x \leq 12$) alloys by magnetization and ^{57}Fe Mössbauer spectroscopy measurements. These alloys show spin glass, reentrant spin glass and ferromagnetic behaviour at different concentrations. The existence of two different Fe local environments is confirmed and they are identified with the low (about $1 \mu_B$) magnetic moment, exclusively Fe coordinated, compressed and on the other hand with the partially Zr coordinated larger volume Fe atoms, respectively. The temperature dependence of the iron hyperfine field distribution can be reproduced by assuming that the compressed Fe atoms are weakly coupled to the rest of the Fe magnetic moments. The high field Mössbauer measurements show that collinear magnetic state was reached in all the alloys below 7 T and the high field susceptibilities deduced from the hyperfine fields are in good agreement with bulk magnetic measurements ruling out the existence of antiferromagnetically aligned Fe moments. The anomalous magnetic properties of these amorphous alloys may be explained by bond percolation: the compressed, low moment Fe atoms are decoupled from the rest of the Fe atoms.

I INTRODUCTION

Sputtered and melt-quenched iron-rich amorphous alloys with less than ≈ 20 at. % of early transition metal (Zr, Hf, Sc, Y, La, Lu, Ce) elements exhibit [1] similar unusual magnetic features. The Curie temperature T_C is strongly decreasing with increasing Fe concentration and eventually the long-range ferromagnetic (FM) order is collapsing. The high-field susceptibility is extremely large, magnetic saturation can not be achieved even in very large applied magnetic fields (30 T). At the highest Fe compositions the low field AC susceptibility shows a cusp characteristic of the paramagnetic-spin glass (PM-SG) transition temperature (T_G), while at lower Fe compositions the typical behaviour of the reentrant spin glasses (RSG) is observed. The susceptibility of this RSG systems decreases sharply from the maximum value attained at T_C , then gradually decreases further with decreasing temperature and suddenly drops off at the "spin freezing" temperature T_f of the FM-SG transition. The pressure dependence of the physical properties of these alloys is also remarkable: besides a significant compressibility, a remarkably large decrease of T_C and an initially increasing T_f with increasing hydrostatic pressure are also obtained.

The atomic structure of these amorphous alloys is little known but they are often considered [2] as amorphous iron stabilized by the inclusion of these early transition metal elements as impurities. In this sense its magnetic behaviour is closely related to that of the hypothetical amorphous iron. The *bcc*, *fcc* and *hcp* polymorphs of crystalline iron exhibit quite different magnetic behaviour depending on the atomic volume of Fe [3]. It seems to be well-documented that the Fe magnetic moment decreases and its magnetic coupling becomes antiferromagnetic when the Fe volume decreases and the coordination number increases. These observations foreshadow the complications regarding the magnetic ground state of the hypothetical amorphous iron which have fluctuations both in the atomic volumes and in the coordination numbers.

Theoretical calculations [4,5,6,7,8] resulted in different

local magnetic moment distributions and magnetic states. The results strongly depend both on the used theoretical approach and on the assumed density of amorphous iron. Kakehashi [4] suggested on the basis of an elaborate temperature dependent itinerant local environmental approximation that amorphous Fe should be a "genuine spin glass", i.e. with a vanishing global moment and with an isotropic distribution of the local magnetic moment directions. According to Krey et al. [5] this spin glass phase competes strongly with the asperomagnetic states (i.e. globally ferromagnetic configurations with randomly frozen transverse spin components), the approximately 0.003 eV per electron energy difference of the two states is within the calculation error.

Experimental data exist only on different iron-rich amorphous alloys since pure amorphous iron was not yet prepared. The most detailed investigations were performed on the amorphous $\text{Fe}_{100-x}\text{Zr}_x$ ($7 \leq x \leq 12$) alloys. In this narrow (6 at.% Zr) composition range a wide variety of different magnetic behaviours is observed. At $x=7$ the transition from the paramagnetic to the SG state is confirmed. The transition in the $x=12$ alloy is characterized as a FM Curie point. In the $8 \leq x \leq 11$ range RSG behaviour, i.e. clear double transitions (PM-FM-SG) are observed [9]. The nature of the developing magnetic states is not well understood. The critical exponents of the PM-FM magnetic phase transition were found in close agreement [10] with the theoretical values for a three-dimensional homogeneous Heisenberg ferromagnet but substantially larger, strongly deviating values [11] indicating the presence of magnetic inhomogeneities were also reported. The critical amplitudes are found [12] to deviate from values theoretically predicted for homogeneous ferromagnets. It is observed by Kaul and Babu [13] that the substitution of Co for Fe in $\text{Fe}_{90-x}\text{Co}_x\text{Zr}_{10}$ alloys significantly increases the fraction of spins actually participating in the phase transition at the Curie point.

The temperature dependence of the AC susceptibility was also interpreted as demonstrating the establishment of long-range ferromagnetic order [14] or as indicating

mictomagnetic behaviour [15]. The observed multicritical point in the concentration dependence is interpreted as the percolation limit of the long range ferromagnetic interactions [16]. Below T_C large (10-50 μm) magnetic domains were observed [17] by Lorentz transmission electron microscopy for $x \geq 8$. On the other hand, small-angle neutron-scattering measurements demonstrated [18] that conventional long-range ferromagnetic order was not achieved at any temperature below T_C . The spin correlation length did not diverge at T_C (or below) but rather remained quite short ($\approx 100\text{-}200 \text{ \AA}$). The presence of relatively large ($\approx 400 \text{ \AA}$) spin clusters which do not disorder above T_C was also seen. Recent small angle neutron scattering in external magnetic field confirmed [19] the existence of significant magnetic scattering in a wide range of length scales. Broad Fe hyperfine field (i.e. magnetic moment) distributions were observed [20,21] in Mössbauer experiments which also show evidence of magnetic inhomogeneities above and below T_C in moderate applied fields ($\approx 3 \text{ T}$).

All proposed explanations of the magnetic anomalies assume the co-existence of ferromagnetic and antiferromagnetic exchange interactions in the system either in the form of spatially separated clusters (antiferromagnetic *fcc*-Fe [22], two-phase two-sublattice model [23] or spin glass regions [17]) or the significant antiferromagnetic exchange is suggested as the cause of the "wandering axis ferromagnet" structure [2,21]. Theoretical calculations [5] predict negative polarization of the Zr atoms in these amorphous alloys supported [24] by indirect evidence based on the pressure dependence of the magnetization and Zr hyperfine field in crystalline Fe_2Zr . On the other hand, the magnetic field dependence of the iron hyperfine field distribution showed [25] no evidence of antiferromagnetic spin alignment. Of course this result does not exclude the presence of antiferromagnetic exchange interactions.

Exchange interactions determine the temperature dependence of the individual magnetic moments via the exchange fields. In amorphous alloys only the distribution of the magnetic moments can be determined through the hyperfine field distribution. The study of the temperature dependence of this iron hyperfine field distribution presents a possibility for investigating the distribution of exchange interactions.

This investigation is the aim of the present paper. The study of the temperature dependence of iron magnetic moment (i.e. hyperfine field) distribution in amorphous $\text{Fe}_{100-x}\text{Zr}_x$ alloys makes it possible to determine in the frame of a molecular field model the standard fluctuation of the nearest neighbour exchange interaction distribution and the correlation between the moment and the exchange interaction distributions. These results, together with the composition dependence of the low temperature hyperfine parameters [26] and with the external magnetic field dependence [27] make it possible to correlate the characteristic features of the local environments in amorphous $\text{Fe}_{100-x}\text{Zr}_x$ alloys with the standard fluctuation and correlation of the relevant nearest neighbour exchange interaction and magnetic moment distributions. The

experimental results will be presented and discussed in three main sub-sections as the low temperature results (A), the temperature dependences (B) and the high field studies (C).

II EXPERIMENTAL

Amorphous ribbons of $\text{Fe}_{100-x}\text{Zr}_x$ ($7 \leq x \leq 12$) were melt spun in vacuum from ingots prepared by induction melting of the pure metals in a cold crucible under argon atmosphere. The absence of crystallinity was confirmed by X-ray diffraction and room temperature Mössbauer spectroscopy. The reproducibility of the sample preparation was good, as the comparison of samples with the same nominal composition, but originating from different batches did show.

Magnetization was measured by a Foner type magnetometer (sensitivity: 10^{-4} emu) in an electromagnet up to 2 T using a flow cryostat between 15 K and room temperature. The Curie temperature was taken to be the kink-point of the magnetization measured in $B_{\text{ext}}=1 \text{ mT}$, while the T_f , T_G values were determined as shown in Fig. 1 applying the same field for all probes.

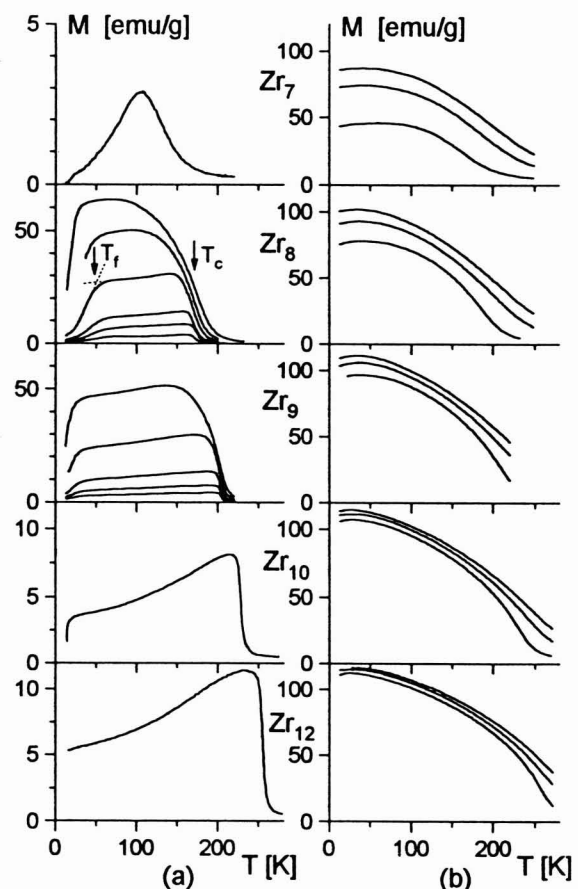


Fig. 1 Temperature dependence of the magnetization of amorphous $\text{Fe}_{100-x}\text{Zr}_x$ alloys in different magnetic fields: $B_{\text{ext}}=1 \text{ mT}$ (a) and 0.1, 0.5 and 1 T (b), respectively. For $\text{Fe}_{92}\text{Zr}_8$ the $B_{\text{ext}}=0.5, 2, 5, 10,$ and 20 mT data, and for $\text{Fe}_{91}\text{Zr}_9$ the $B_{\text{ext}}=0.5, 2, 5,$ and 10 mT data are also shown. The definition of the spin freezing temperature T_f and the Curie temperature T_c is also indicated.

Mössbauer spectra were obtained by a conventional constant-acceleration spectrometer with 1.8 GBq $^{57}\text{CoRh}$ source at room temperature. Polarized spectra were obtained in a flow-cryostat by cooling the sample from room temperature in a magnetic field of $B_{\text{ext}}=13$ mT applied parallel to the sample plane (i.e. perpendicular to the γ -direction), using a small permanent magnet. For the $T=4.2$ K measurements the samples were immersed into liquid helium. In this case the polarized spectra are taken on zero field cooled samples. Mössbauer measurements were also performed in external magnetic fields applied parallel to the γ -beam using a 7 T Janis superconducting magnet.

For the evaluation of the spectra the binomial distribution method [28] was used where the shape of binomial distributions is adjusted to the spectra and linear correlation is assumed between the hyperfine field, isomer shift and quadrupole splitting. The effect of the uncorrelated part of the isomer shift and quadrupole splitting distribution was taken into account in the linewidth of the individual six lines, which together with $I_{2,5}$, the relative intensity of the 2-5 lines was also determined by iteration. In the present evaluations two binomial sets were used.

III RESULTS AND DISCUSSION

The magnetization curves of Fig. 1(a) show the same characteristic features also observed in Refs. [9, 15 and 29]: PM-SG transition for $x=7$, double PM-FM-SG transition (RSG behaviour) for $x=8, 9$ and 10, PM-FM transition for $x=12$. The composition dependence of the transition temperatures (T_C : PM-FM, T_f : FM-SG and T_G : PM-SG) shown in Fig. 2 are also in good agreement with the literature values. When T_f is determined by magnetic measurements in weak external fields it slightly increases

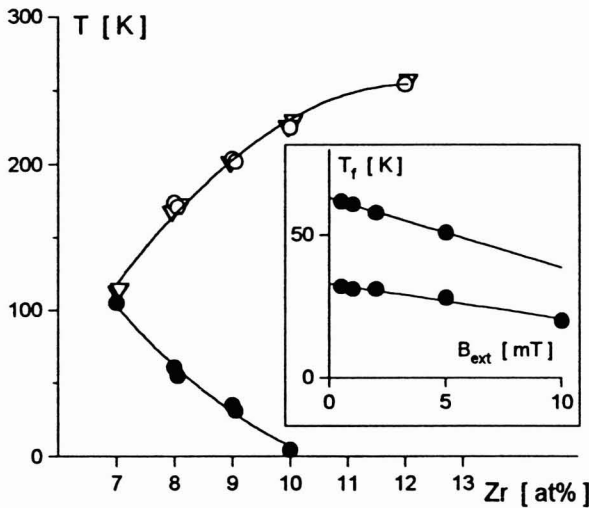


Fig. 2 Concentration dependence of the Curie temperatures, T_C (empty symbols) and of the spin freezing temperatures, T_f (dots) in $\text{Fe}_{100-x}\text{Zr}_x$ glasses, determined from the magnetic (circles) and from the Mössbauer (triangles) measurements, respectively. For $\text{Fe}_{93}\text{Zr}_7$ only the PM-SG transition (T_G is the cusp temperature) was observed. The insert shows the magnetic field dependence of T_f for $x=8$ and 9 at.% Zr, respectively.

with decreasing B_{ext} (see the insert of Fig. 2), the values extrapolated to $B_{\text{ext}}=0$ are shown. The T_C values determined from the magnetization and from the temperature break of the full halfwidth of the Mössbauer spectra agree well with each other. The T_f values were also determined by Mössbauer spectroscopy under the influence of a strong external magnetic field. Their relation to the T_f values determined by magnetic measurements in much weaker field will be discussed below in sub-section B.

A. Low temperature Mössbauer results

Typical Mössbauer spectra measured at 4.2 K in small external field applied in the plane of the samples (perpendicular to the direction of the gamma-rays) are shown in Fig. 3. The 12 and 10 at.% Zr samples are easily polarized which is indicated by the large increase of the intensities of the 2-5 lines of the spectra. The influence is smaller for the investigated 9 at.% Zr sample. The 8 and 7 at.% Zr samples on the other hand show no detectable polarization in small external fields. 12 hours annealing at 500 K of the 8 at.% Zr sample did not improve the polarizability at 4.2 K but it has resulted in an increased polarization at 77 K leaving the Mössbauer parameters otherwise unchanged.

The hyperfine field distributions evaluated from these spectra are shown in Fig. 4. They are rather similar to those

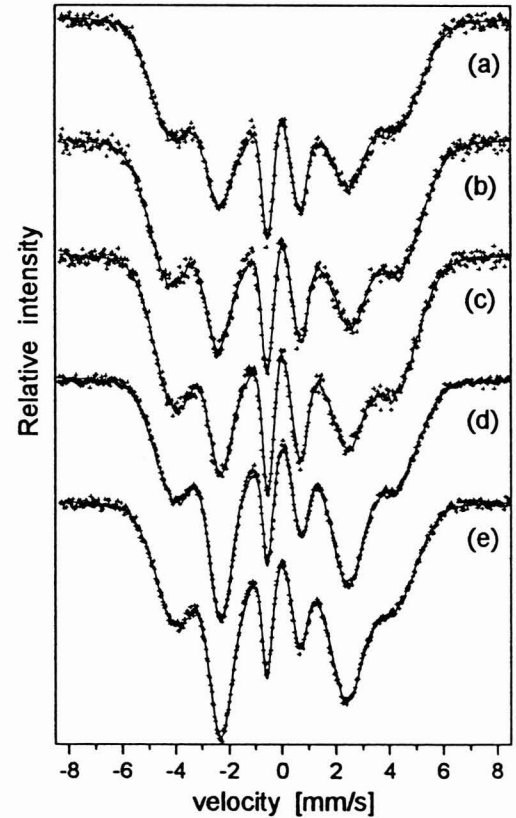


Fig. 3 Typical Mössbauer spectra of amorphous $\text{Fe}_{100-x}\text{Zr}_x$ alloys ($x=7$ (a), $x=8$ (b), $x=9$ (c), $x=10$ (d) and $x=12$ (e), respectively) measured at 4.2 K in $B_{\text{ext}}=13$ mT applied parallel to the sample plane.

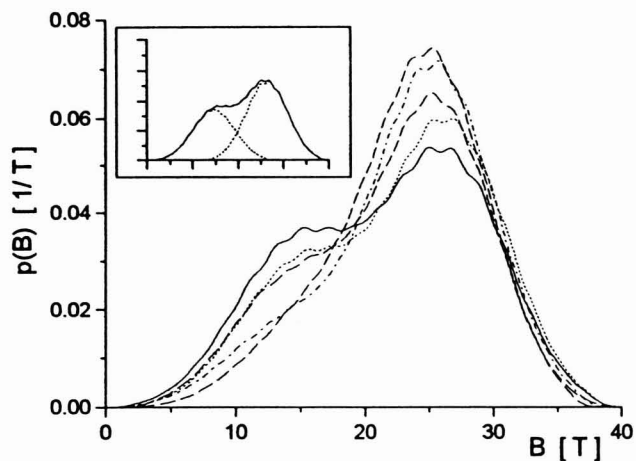


Fig. 4 Hyperfine field distributions of amorphous $\text{Fe}_{100-x}\text{Zr}_x$ alloys at 4.2 K. ($x=7$ continuous line, $x=8$ dotted line, $x=9$ broken line, $x=10$ dot-dashed line, $x=12$ dashed line). The insert shows the decomposition of the $p(B)$ of $\text{Fe}_{93}\text{Zr}_7$ into two distributions representing the high field and low field contributions, respectively.

obtained in Refs. [22, 25, 30-33] in a narrower composition range. Their characteristic feature is the low-field shoulder or peak besides the high-field peak. Unfortunately, the 2-5 lines of the spectra of these high-field components overlap with the 1-6 lines of the low-field components making it

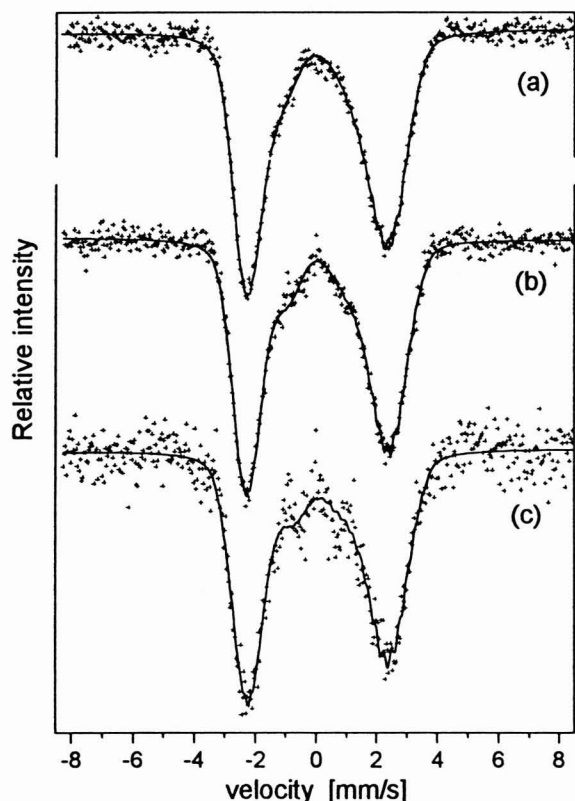


Fig. 5 The separated 2-5 lines of the spectra of amorphous $\text{Fe}_{100-x}\text{Zr}_x$ at 4.2 K obtained by the spectrum subtraction method [28] ($x=12$ (a), $x=10$ (b) and $x=9$ (c), respectively). The solid lines are the least-square fitted curves.

more difficult to avoid evaluation artifacts. The spectrum subtraction method [28] confirms our evaluation. The separated 2-5 lines of the spectra are shown in Fig. 5 and their shape presents directly the calculated increase in the intensity of the low field components for decreasing Zr content. Similar separated 2-5 lines were obtained [34,35] earlier in the case of $\text{Fe}_{90}\text{Zr}_{10}$. The poor statistics of $\text{Fe}_{91}\text{Zr}_9$ is due to the weaker polarizability of the sample. It altogether prevents the proper separation of the 2-5 lines for $\text{Fe}_{92}\text{Zr}_8$ in small fields.

The hyperfine field distributions can be separated [22,31] into high-field (HF) and low-field (LF) contributions as

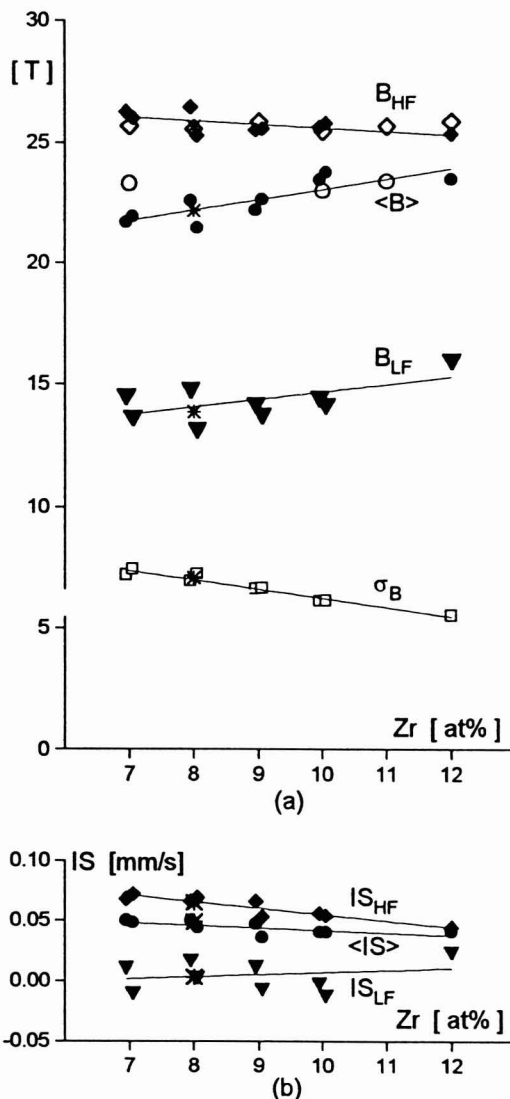


Fig. 6 The concentration dependence of the average hyperfine field $\langle B \rangle$ (dots), the high field B_{HF} (diamonds), the low field B_{LF} (triangles) components and the standard deviation of the hyperfine field distribution σ_B (a) and the average isomer shift $\langle \text{IS} \rangle$ (dots), the isomer shifts of the high field IS_{HF} (diamonds) and low field IS_{LF} (triangles) components (b), respectively, measured at 4.2 K. The star represents these values for the heat-treated (at 500 K for 12 hours) sample. Published values of the average hyperfine field are also shown: empty diamonds (Ref. [2]) and circles (Ref. [43])

shown in the insert of Fig. 4. The composition dependence of these parameters (the peak values of the hyperfine fields B_{HF} and B_{LF} , and the isomer shifts IS_{HF} and IS_{LF} , respectively) and the average values of the isomer shifts $\langle IS \rangle$, hyperfine fields $\langle B \rangle$ and the standard widths of the distribution, σ_B are shown in Fig. 6. The literature data also shown in Fig. 6 will be discussed at the end of this subsection. Fig. 7 contains the relative intensity of the low field component p_0 as a function of Zr concentration, the data are in good agreement with the values obtained in Refs. [22 and 31].

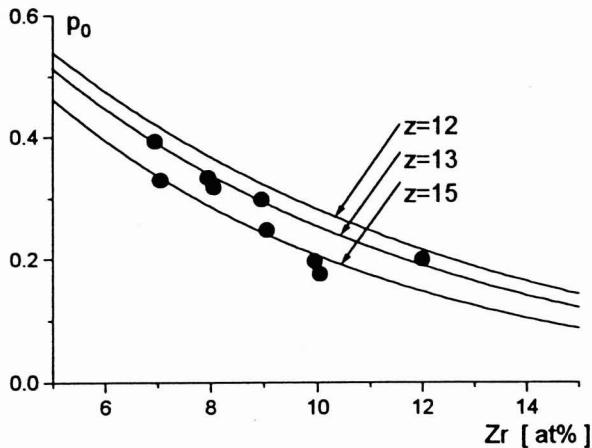


Fig. 7 The concentration dependence of the relative intensity of the low field component p_0 . The solid lines represent the proportion of iron atoms, having iron nearest neighbours only for a random alloy with coordination numbers $z=12, 13$ and 15 , respectively.

The atomic structure of amorphous $Fe_{90}Zr_{10}$ has been investigated by conventional X-ray diffraction [36] and also by the anomalous scattering technique [37,38], by EXAFS [39] and by XANES [40]. The coordination numbers for an Fe atom (obtained [37,38] from the partial distribution functions in the two investigations) were 11.8 Fe atoms and 1.4 Zr atoms, and 10.2 Fe atoms and 1.6 Zr atoms, respectively, giving as total coordination number 13.2 and 11.8 atoms. The Fe coordination number of a Zr atom was found [38] to be 14.5. Computer models show [40] a wide distribution of coordination numbers, for example the Fe-Fe coordination number spans the range from 8 to 16. The experimentally determined average interatomic distances extend [36,38,39] from 2.42 to 2.63 Å for the Fe-Fe distances and from 2.69 to 2.83 Å for the Fe-Zr distances. EXAFS investigation [39] of a heat-treated (at 623 K for 3 Ks) sample indicated the presence of two kind of Fe-Fe pairs: one with high Fe coordination and short Fe-Fe distance (2.39 Å) the other with larger Fe-Fe distance (2.55 Å), respectively.

The decomposition of the hyperfine field distribution into high- and low-field contributions, corresponds to the presence of two kind of Fe atoms. As it will be discussed below the Fe atoms with low hyperfine field, i.e. with smaller magnetic moment should be associated to the atomic environments with only Fe nearest neighbours [22].

In the absence of detailed information on the short range order of these alloys the ratio of these low moment Fe atoms is approximated as $(1-x/100)^z$, i.e. the probability of having no solute nearest neighbours in a random solid solution of coordination number z . The calculated curves for $z=12, 13$ and 15 are shown in Fig. 7 and they approximate reasonably the observed composition dependence of p_0 . The magnetic moment of these Fe atoms is about $1 \mu_B$ using [2] the value of $14.5 T/\mu_B$ for the proportionality constant between the hyperfine field and magnetic moment.

The isomer shifts of the two components, IS_{LF} and IS_{HF} were determined by using the assumption of linear correlation between hyperfine field and isomer shift. IS_{LF} was found to be lower by about 0.08 mm/s than IS_{HF} . Inspection of the separated 2-5 lines in Fig. 5 shows directly the evaluated trend: the asymmetry of the inner parts follows that of the main peaks. The more negative isomer shift of the Fe sites with Fe nearest neighbours only is quite unexpected on the basis of the known composition dependence [41] and thus it must be related to their decreased average volume. On the base of the pressure dependence [42] of the isomer shift, an assumed 10% decrease in the relative volume of *bcc* Fe decreases the isomer shift by 0.14 mm/s, that of the *hcp* Fe by 0.08 mm/s, respectively. Thus the deduced isomer shift difference between HF and LF Fe atoms suggests an approximate 10% decrease in the average atomic volume of Fe when it has no Zr nearest neighbours. This result is in line with the forementioned EXAFS [39] investigation. According to the isomer shift data the average atomic volume of the LF Fe atoms slightly increases with increasing Zr content resulting in a small increase of their magnetic moments, i.e. B_{LF} is also increasing. Both B_{HF} and IS_{HF} are decreasing with increasing Zr content which is expected for iron atoms surrounded by Zr neighbours on the base of the observed concentration dependences of sputtered samples in a wider composition range [41]. However, in the investigated region the mean hyperfine field $\langle B \rangle$ increases slightly for increasing Zr concentration which is mainly caused by the decrease of the low field fraction.

The low temperature iron hyperfine field distributions determined in the present work are in excellent agreement with the theoretical calculations of Krey et al. [5] including details like the composition dependence of the high field component. On the other hand, the extrapolation of the present results to the case of amorphous iron do not support the results of Kakehashi [4] which would predict a dominant nonmagnetic contribution instead of the extrapolated experimental result, the $\approx 1 \mu_B$ magnetic moments. Also his calculated magnetic moment distribution is getting sharper when the SG state is attained from the RSG state contrary to the increase of σ_B found in the present experiments. Similarly, the calculated magnetic moment distribution of Xu et al. [6] results in an appreciable amount of high moment tail not observed in the present experiments.

The reliable calculation of magnetic moment distribution in amorphous alloys is not a simple task even with the most advanced computer techniques. Recent calculations [8]

predict antiferromagnetically aligned moments both, for Fe-rich Fe-B and Fe-Zr alloys, while neither the characteristic anomalous magnetic behaviour nor the double peaked hyperfine field distribution of the Fe-Zr type alloys are observed experimentally for the Fe-B alloys. Although it might be assumed that the different experimental behaviour of the Fe rich Fe-B and Fe-Zr alloys is only connected to the fact, that the composition range of anomalous magnetic behaviour is not yet attained in the Fe-B system, the agreement between theory and experiment is far from being assuring.

A recent publication [43] questions altogether the reality of the double peak structure of the hyperfine field distributions in Fe rich amorphous alloys and attributes it to evaluation artifacts. It is well-known [44] that in the case of broad hyperfine field distributions strong correlation is observed between the value of the *a priori* unknown 2-5 line intensities and the shape of the evaluated distribution due to the overlap of the lines. Shape independent procedures for the Fourier decomposition like Window's method [45] are more sensitive for this type of correlation than those which use flexible shape like the binomial distribution method [28] applied in the present work. It means that extreme precaution is necessary in the proper evaluation of the broad Mössbauer spectra characteristic of the investigated alloys. The difficulties are well illustrated by the observation that the recently published [43] average hyperfine field values agree well with our values [26] shown in Fig. 6 which take into account the low field part of the distribution, while the 10% larger average values published earlier [2] correspond well to our high field components B_{HF} , i.e. in that case the low field part of the distribution was neglected.

While the possibility of a non-physical multiple-peak structure due to the improper evaluation of Mössbauer spectra is well established it is beyond any doubts that it is not the case in the Fe-Zr system. Besides the systematic composition dependence of the double peak structure discussed above, the established common temperature dependence of both peaks at low temperatures (see sub-section B) and also the systematic external magnetic field dependence ([27] and sub-section C.) proves the reality of the double peaked hyperfine field distributions.

Between 12 and 9 at% Zr content the shoulder corresponding to the asymmetrical hyperfine field distributions can be seen directly on the 2-5 Mössbauer lines (Fig.5) when the overlap with the outer and inner lines are removed by the linear combination of two spectra. It is only possible when small applied field results in a considerable polarization of the spectrum. The same procedure can be applied even at 7 at% Zr concentration - only in this case much larger external field is necessary to obtain the necessary polarization (as it will be shown in sub-section C.) resulting in even stronger asymmetric shoulder of the 2-5 lines. These results directly support the observed 30% increase in σ_B between 7 and 12 at% Zr content (Fig.6).

A further convincing proof of the two peak structure of the relevant hyperfine distributions is however the independent detection of both peaks in nuclear magnetic resonance

(NMR) experiments [46], where the hyperfine field distribution is directly observed and the inversion problem so apparent in Mössbauer spectroscopy is absent. While the determination of the hyperfine field distribution by NMR is also somewhat complicated due to domain wall enhancement problems, the existence of a double peaked hyperfine field distribution in good agreement with the majority of published results is confirmed. Our investigations on the other hand do not support the view [47] that the distribution is properly evaluated by using two independent symmetric gaussians. Our experiences show that the use a flexible form, e.g. the double binomial utilized in our work, is inevitable for the reliable determination of the hyperfine field distribution of this type of amorphous alloys. It should also be remarked that in contrast to the claim [43] that only Mössbauer evaluations hint to any kind of magnetic non-uniformities a recent small angle neutron scattering work [16] also confirms the existence of anomalous magnetic scattering in Fe rich Fe-Zr alloys.

B. Temperature dependence of the hyperfine field distribution

The character of the magnetic exchange interactions can be studied via the temperature dependence of the individual magnetic moments which is reflected in the iron hyperfine field distribution $p(B)$. Typical Mössbauer spectra and hyperfine field distributions as a function of temperature are shown in Figs. 8-10. Characteristic features include the

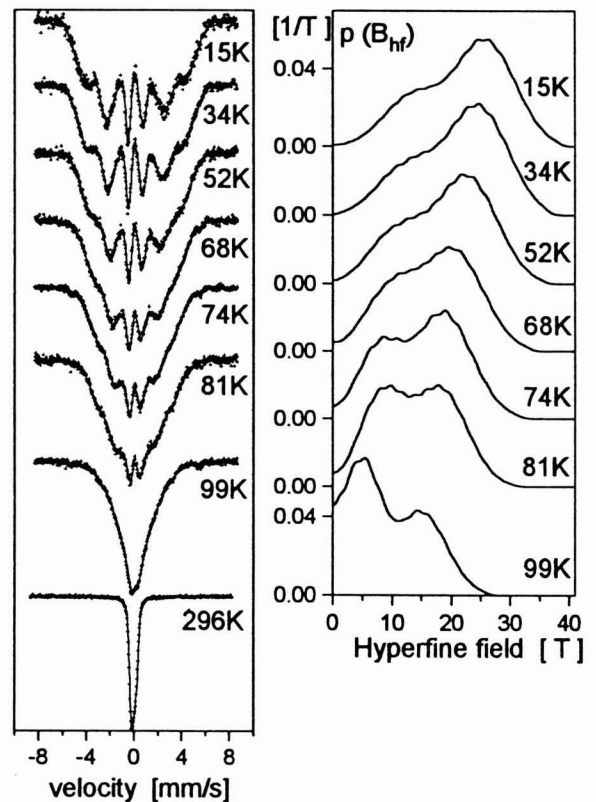


Fig. 8 Temperature dependence of the Mössbauer spectra and hyperfine field distributions for amorphous $Fe_{93}Zr_7$. The room temperature spectrum is also shown.

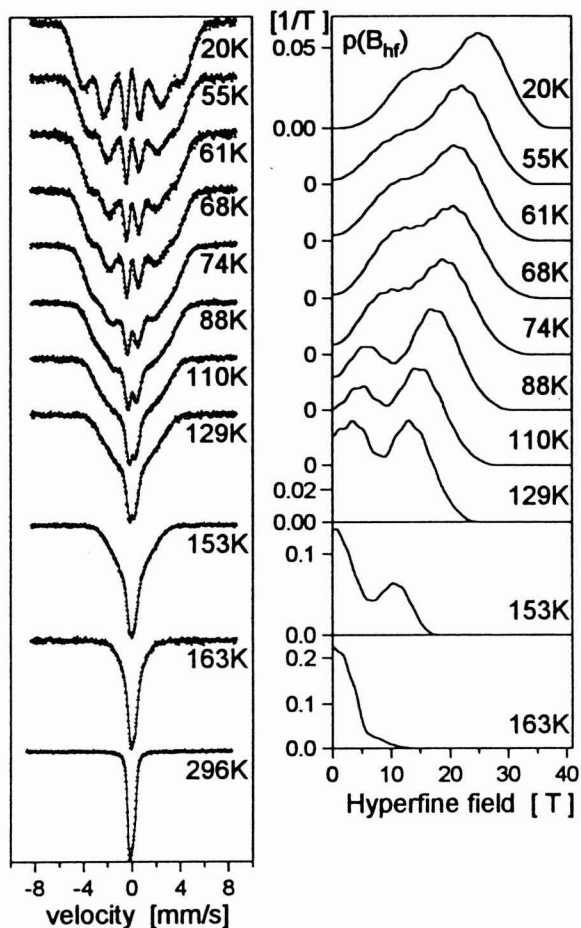


Fig. 9 Temperature dependence of the Mössbauer spectra and hyperfine field distributions for amorphous $\text{Fe}_{92}\text{Zr}_8$. The room temperature spectrum is also shown.

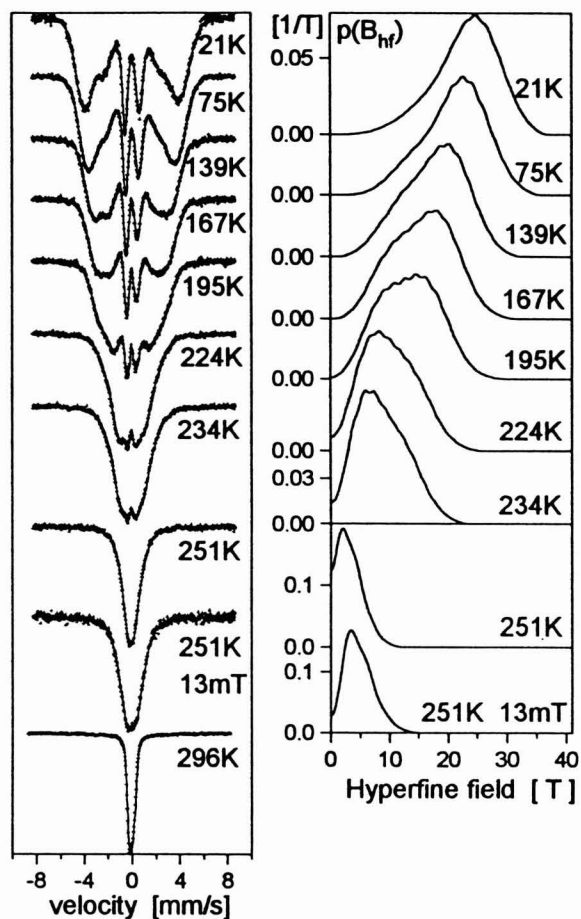


Fig. 10 Temperature dependence of the Mössbauer spectra and hyperfine field distributions for amorphous $\text{Fe}_{88}\text{Zr}_{12}$. The spectrum and $p(B)$ measured in an external field of 13 mT applied parallel to the sample plane at 251 K and the room temperature spectrum is also shown.

decreased intensity of the 2-5 lines both in the FM state of the RSG $\text{Fe}_{92}\text{Zr}_8$ and in the FM $\text{Fe}_{88}\text{Zr}_{12}$ due to the stresses between the sample and the adhesive tape which results in a magnetic polarization perpendicular to the sample plane (parallel to the gamma-rays) induced by the positive magnetostriction. In the SG state of $\text{Fe}_{92}\text{Zr}_8$ some resemblance to this behaviour still remains, since the intensity ratio of the 2-5 lines to the 3-4 lines is lower than 2, the value which is expected for random spin orientations. Similar result was reported [35] for the RSG $\text{Fe}_{90}\text{Zr}_{10}$. The SG $\text{Fe}_{93}\text{Zr}_7$ has almost random spin configurations, here the observed ratio, $I_{2,5}$ is around 1.9.

Near to the paramagnetic transition the spectra of the SG and RSG samples show in a wide (more than 30 K) temperature range broad, rather symmetric, peaked feature (Figs. 8(b) and 9(b)) characteristic of magnetic spin relaxation. The FM $\text{Fe}_{88}\text{Zr}_{12}$ shows a similar behaviour in a substantially narrower range (10 K). In this temperature region the spectra are extremely sensitive for small external field ($B_{\text{ext}}=13$ mT in [48]) proving the existence of magnetic cluster relaxation. An example is shown for $\text{Fe}_{88}\text{Zr}_{12}$ in Fig. 10(b). No appreciable effect of the small B_{ext} was found below $T/T_c \approx 0.8$ in agreement with the results of the cluster relaxation fits [49] to the spectra.

An interesting feature of the evaluated hyperfine field distributions is the increase in the intensity of the low field component above $T/T_c \approx 0.6$. Its insensitivity to small applied B_{ext} below $T/T_c \approx 0.8$ excludes the relaxation as its origin and thus it should be considered as the result of the temperature dependence of the individual magnetic moments: due to small exchange fields some high field components decrease much faster with increasing temperature than the average, causing the apparent increase in the amount of the low field contribution. This indicates that separate handling [30,31,47] of the high and low field peaks of $p(B)$ at high temperatures is problematic.

The reduced average hyperfine fields $\sigma(T) = \langle B(T) \rangle / \langle B(0) \rangle$ are shown in Fig. 11. Our data for $x=9$ are in good agreement with the measurement of Ghafari et al. [20] but disagree with the results of Ryan et al. [2,21] for $x=7, 8$ and 9. In the case of $x=10$ the overall agreement is satisfactory with Ref. [32]. The most remarkable feature of the $\sigma(T)$ curves is the change from the usual convex shape of $x=12$ (FM system) and $x=10$ to the concave form of $x=9$ and 8 (RSG systems) and then to change back again to the convex shape for $x=7$ (SG system). Similar change in the $\sigma(T)$ shapes was reported e.g. for the FM-RSG transition [50] in crystalline FeNiMn and for the SG-RSG transition

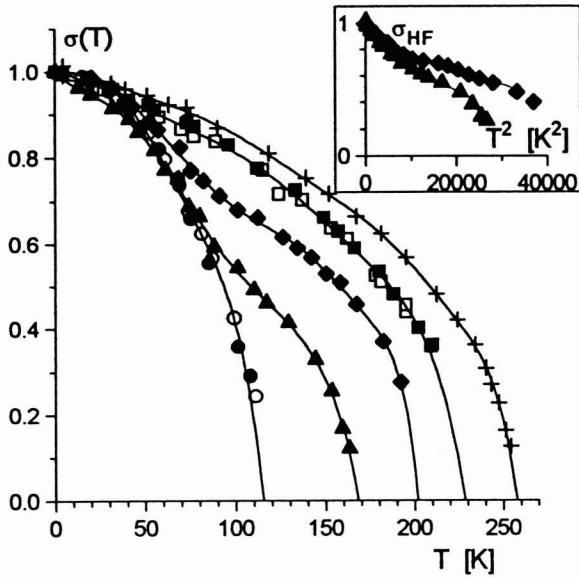


Fig. 11 The reduced average iron hyperfine field $\sigma(T)=\langle B(T) \rangle / \langle B(0) \rangle$ as a function of temperature for amorphous $\text{Fe}_{100-x}\text{Zr}_x$ ($x=7$ and 10 : for two different samples empty and full circles and squares, respectively; $x=8$: full triangles; $x=9$: rhomb; $x=12$: cross). The proper symbols in triangles are the $\sigma(T)$ values in $B_{\text{ext}}=13$ mT. The continuous lines are guides to the eye.

[51,52] in amorphous RuFeB and FeScZr alloys as a function of composition.

The unusual increase in the reduced average hyperfine field $\sigma(T)$ at low temperatures is a characteristic feature of the RSG systems. Typical explanations of this behaviour include chemical segregation or spin canting transition. In our case the temperature anomaly has occurred at around 85 K for both $x=8$ and 9 alloys. This temperature is significantly higher than the T_f values observed in the magnetization measurements (Fig. 2). The temperature of spin freezing as a function of external magnetic fields can be determined from the disappearance of the 2-5 lines. The $T_f(B_{\text{ext}})$ dependence follows a linear relationship for $\text{Fe}_{93}\text{Zr}_7$ with a slope of about -22 K/T. The value of T_f extrapolated for $B_{\text{ext}}=0$ agrees well with the value measured by magnetic methods in small external fields. Correction of the applied field with the demagnetization field leaves the linear relationship practically unchanged, but the slope is a somewhat more negative value (about -25 K/T). The shape of $T_f(B_{\text{ext}})$ changes as a function of the Zr content and it can be well approximated by a $(B_{\text{ext}})^{2/3}$ functional form for $\text{Fe}_{91}\text{Zr}_9$. The composition dependence of the T_f values determined directly from the $I_{2,5}(B_{\text{ext}})$ dependences follows the trend observed in the magnetization measurements: they decrease with increasing Zr content, only the Mössbauer values are substantially higher [55]. Some of the problems of the $T_f(B_{\text{ext}})$ determination at high temperatures ($80 \text{ K} \leq T$) may be related to the magnetic relaxation effects resulting in a large increase of the magnetization in external magnetic field [48].

The unusual increase of the hyperfine field for both

compositions at about the same temperature seems at the first glance to support the explanation based on a supposed magnetic phase separation [22,23,53] where the critical (Néel or Curie) temperature would correspond to the temperature of the anomaly. The absence of any significant amount of paramagnetic contribution at higher temperatures and the result that the high field component B_{HF} shows the same type of anomaly (see the insert of Fig. 11 and Ref. [33]) rules out the before mentioned possibility. Indeed, these observations indicate that all iron atoms contribute to the temperature anomaly, it cannot be associated with a given type, for example the iron-rich, environments. Since all iron magnetic moments participate in the anomalous $\sigma(T)$ behaviour it is very attractive to attribute [30,31] it to the broad distribution of the exchange integrals, to the presence of weakly coupled magnetic moments which have distorted magnetization curves. However, it is difficult to reconcile this kind of explanation with the observed composition dependences: for $x=7$ even larger anomaly would be expected instead of its disappearance.

The spin canting model [54] attributes the increase of $\langle B(T) \rangle$ when extrapolated to 0 K from the low ($T < T_f$)

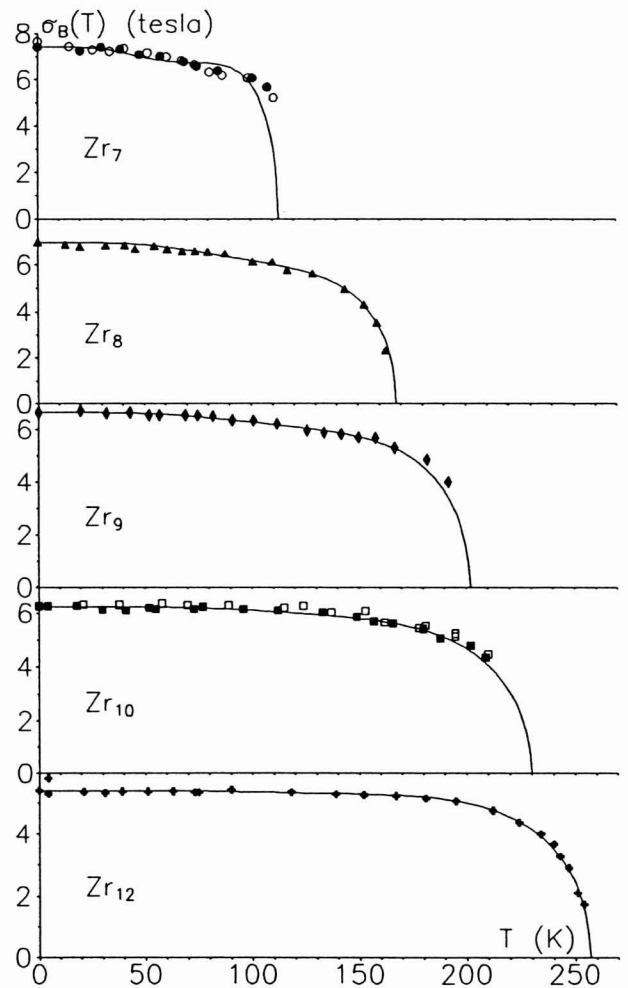


Fig. 12 Temperature dependence of the standard deviation of the hyperfine field distribution σ_B of amorphous $\text{Fe}_{100-x}\text{Zr}_x$.

instead of the high ($T > T_f$) temperature ranges, to the freezing of the transversal components of the magnetic moments. According to theoretical calculations for the $\text{Fe}_{100-x}\text{Zr}_x$ system the weakly concentration dependent magnitude of the transverse polarization is typically 0.3 to $0.4 \mu_B$ yielding only about 4% larger total magnitude than the global z-polarization [5]. It is difficult to explain with this model the strongly composition dependent large experimental values ($\approx 30\%$ for $x=8$ and $\approx 20\%$ for $x=9$).

The standard widths, σ_B of the hyperfine field distributions shown in Fig. 12 decrease monotonously with increasing temperature. They do not reflect the anomalous temperature dependence of the reduced hyperfine field, $\sigma(T)$ for $\text{Fe}_{92}\text{Zr}_8$ and $\text{Fe}_{91}\text{Zr}_9$. In the transverse spin freezing model [54] the value of the average hyperfine field $\langle B \rangle$ extrapolated to 0 K from the high ($T > T_f$) temperature range is smaller than the value extrapolated from the low ($T < T_f$) temperature region. The increase in the extrapolated value of $\langle B \rangle$ is attributed to the contribution of the frozen transversal components of the magnetic moments at low temperatures which would average out at higher temperatures. If this explanation were valid, a similar increase would also be expected for the width of the distributions σ_B , which is not observed.

The temperature dependence of σ_B can be interpreted within the framework of a simple model [56]. In the molecular field approach the average spin (i.e. the magnetic moment) at the i -th site S_i at temperature T is given by

$$\langle S_i \rangle_T = S_i B_S \left(\frac{S_i}{kT} \sum_{j=1}^z J_{ij} \langle S_j \rangle_T \right) \quad (1)$$

where B_S is the Brillouin function of spin quantum number S_i , J_{ij} is the exchange integral between the sites i and j and the j -summation runs over all z nearest neighbours. Since in the investigated systems we have a distribution of the magnetic moments instead of the discrete values of S_i , equation (1) is extended for continuous S_i values, where

$$S = \frac{1}{N} \sum_{i=1}^N S_i, \quad \text{the average of the magnetic moments at } T=0\text{K}$$

(N denotes the total number of spins). The relative fluctuation in the magnetic moment, s , in the exchange integral, j , and the correlation, k , between the magnetic moment and the exchange interaction distributions is described respectively as

$$s^2 = \frac{1}{N} \sum_i s_i^2, \quad j^2 = \frac{1}{N} \sum_i j_i^2 \quad \text{and} \quad k = \frac{1}{N} \sum_i s_i j_i \quad (2)$$

where $S_i = S(1+s_i)$, $\sum_j J_{ij} = zJ(1+j_i)$, J is the average exchange interaction: $J = (1/Nz) \sum_{ij} J_{ij}$, $\sum_i s_i = 0$, $\sum_i j_i = 0$, $-s_j \leq k \leq s_j$. It is worth to emphasize, that j measures the fluctuation of the quantity $\sum_j J_{ij}$ and is not equal to that of the individual exchange interactions. Thus, via the value of j it is also possible to take into account also the fluctuations in z , i.e. in the number of nearest neighbours characteristic to amorphous alloys. The relative width of the hyperfine field distribution at $T \approx 0\text{K}$, i.e. $s \approx \sigma_B(4.2\text{K}) / \langle B(4.2\text{K}) \rangle$ makes possible a direct measurement of s .

Assuming $|s_i| \ll 1$, $|j_i| \ll 1$ and performing Taylor expansion

of equation (1) to second order of s_i and j_i we obtain the temperature dependence of the relative width of the magnetic moment distribution as given by

$$\left(\frac{\delta\sigma(\tau)}{S\sigma(\tau)} \right)^2 = s^2 + (s^2 + j^2 + 2k) \left(\frac{B'_S(\sigma/\tau)}{\tau} \frac{3S}{S+1} \right)^2 + 2(s^2 + k) \left(\frac{B'_S(\sigma/\tau)}{\tau} \frac{3S}{S+1} \right) \quad (3)$$

where $(\delta\sigma(\tau))^2 = \frac{1}{N} \sum_i (S_i \sigma_i(\tau) - S\sigma_0(\tau))^2$ is the width of the magnetic moment distribution. $\tau = T/T_c$, σ_i and σ_0 are the values of the reduced magnetization, respectively. The functional form will only be temperature independent if $s^2 = j^2 = -k$. In this case the width of the magnetic moment distribution follows the temperature dependence of the average magnetic moment.

Fig. 13 shows typical calculated curves of the temperature dependence of the standard width of the magnetic moment distribution. It is clear that a hump is expected around $T/T_c \approx 0.8$ which is suppressed only by a strong correlation between the magnetic moments and their interaction strengths. The magnitude of the hump is larger for larger

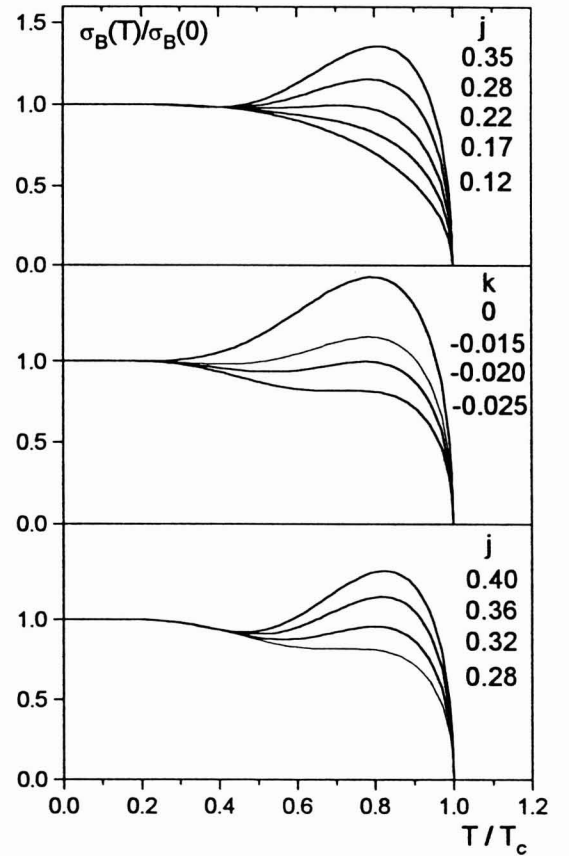


Fig. 13 Typical temperature dependence of σ_B calculated for different set of parameters: j-dependence for $s^2 = k = 0.015$ (a); k-dependence for $s^2 = 0.015$, $j^2 = 0.08$ ($j = 0.28$) (b); and j-dependence for $s^2 = 0.015$, $k = -0.025$ (c).

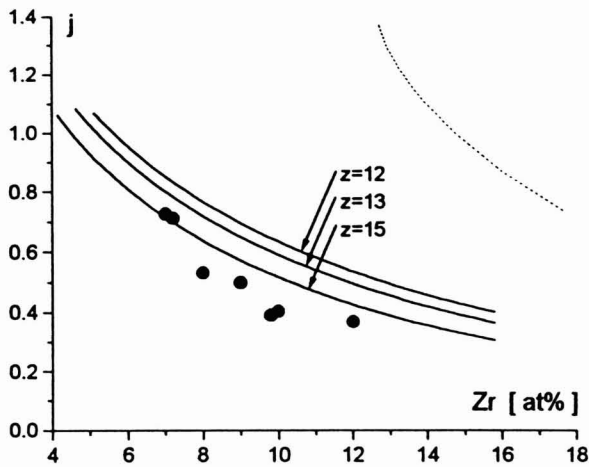


Fig. 14 The standard fluctuation of the nearest neighbour exchange interaction, j around the reduced average value as a function of Zr content in amorphous $\text{Fe}_{100-x}\text{Zr}_x$. The continuous and broken curves are calculated in the simple models explained in the text.

fluctuation of the exchange integrals and the peak value strongly determines the two free parameters of the model.

The calculated and experimentally determined temperature dependences of $\delta\sigma$ are compared in Fig. 12 where $\sigma_B(T) = [\langle B(0) \rangle / S] \delta\sigma(T)$. The overall agreement is good, when the two free parameters j and k , (the standard fluctuation of the exchange interaction distribution and its average correlation with the magnetic moment distribution) are determined by the normal least squares fitting procedure.

The deduced standard fluctuation of the nearest neighbour exchange interaction, j around the reduced average value are shown in Fig. 14.

The observed composition dependence of j can be reproduced by a random model. In line with the low temperature Mössbauer results the existence of two kind of Fe sites with different exchange interactions is assumed: the iron atoms with Zr nearest neighbours are treated by a single ferromagnetic coupling J_0 , while the iron atoms surrounded exclusively by other Fe atoms are supposed to be fully decoupled: their coupling is taken to be zero. Random distribution of Zr atoms with different possible coordination numbers, z results in the continuous calculated curves of Fig. 14. On the other hand, if the Fe atoms surrounded exclusively by Fe neighbours would be antiferromagnetically coupled a much stronger compositional increase of j would be expected for decreasing Zr content. The broken line in Fig. 14 shows the result of the calculation where $-J_0$ was used for the value of the hypothetical antiferromagnetic coupling.

C. High field Mössbauer results

The temperature dependent Mössbauer measurements give no evidence for the presence of any substantial amount of antiferromagnetic exchange interactions in these systems. Further support for the absence of antiferromagnetically aligned Fe moments was obtained from the studies performed in external magnetic fields.

In magnetically split spectra the relative intensity of the second and fifth lines is given by $I_{2,5} = 4\sin^2\Theta / (1 + \cos^2\Theta)$, where Θ is the angle between the magnetic moment and the magnetic field, B_{ext} applied parallel to the gamma beam direction (i.e. perpendicular to the surface of the sample). A random Fe spin orientation corresponds to the value of $I_{2,5} = 2$. In the case when all magnetic measurements are collinear to B_{ext} (i.e. for complete magnetic saturation) $I_{2,5} = 0$.

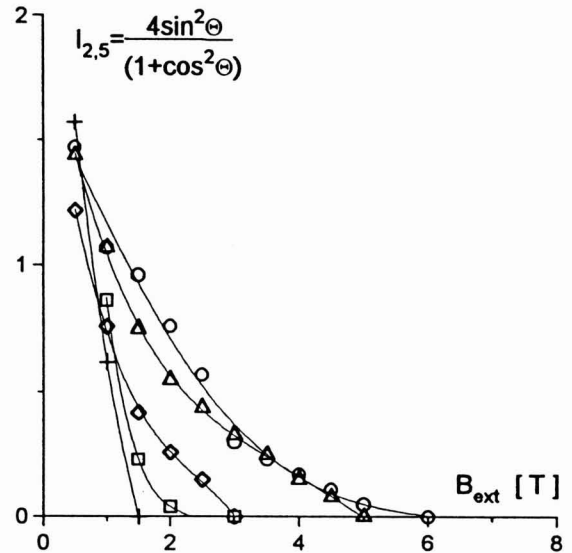


Fig. 15 Relative intensities of the 2-5 lines, $I_{2,5}$ measured at 4.2 K for the amorphous $\text{Fe}_{100-x}\text{Zr}_x$ alloys ($x=7$ circles, $x=8$ triangles, $x=9$ rhombs, $x=10$ squares, and $x=12$ crosses) are shown as the function of the external field. The continuous lines are guides to the eye.

It was found that the collinear magnetic state was reached in all investigated alloys below 6 T [27]. The values of $I_{2,5}$ are summarized in Fig. 15 as a function of the Zr content and B_{ext} . In this figure the values of B_{ext} were not corrected for the demagnetization effects which results in about 1.2 T demagnetization fields in this geometry and in these applied magnetic fields. The strong decrease of $I_{2,5}$ even in relatively small applied fields (smaller than the demagnetization field) is especially remarkable. Fig. 16 shows the typical Mössbauer spectra in this case for $\text{Fe}_{93}\text{Zr}_7$. Since the internal field is practically zero (the applied field is compensated by the demagnetization field), the splitting of the spectrum in 1 T external field is not influenced by the applied field, only the value of $I_{2,5}$ has decreased by a factor of two. The considerable difference in the $I_{2,5}$ intensities allows the separation of the 2-5 lines of the spectra which was not possible in small applied fields. Fig. 16 shows the result which is obtained from the linear combination of the two spectra eliminating the outer (1-6) and inner (3-4) lines. The shape of the separated 2-5 lines confirms directly the evaluated hyperfine field distribution shown in Fig. 4.

The Fe hyperfine field is approximately proportional [2] to the absolute value of the Fe magnetic moment with a conversion factor of about $14.5 \text{ T}/\mu_B$ and it is known to be

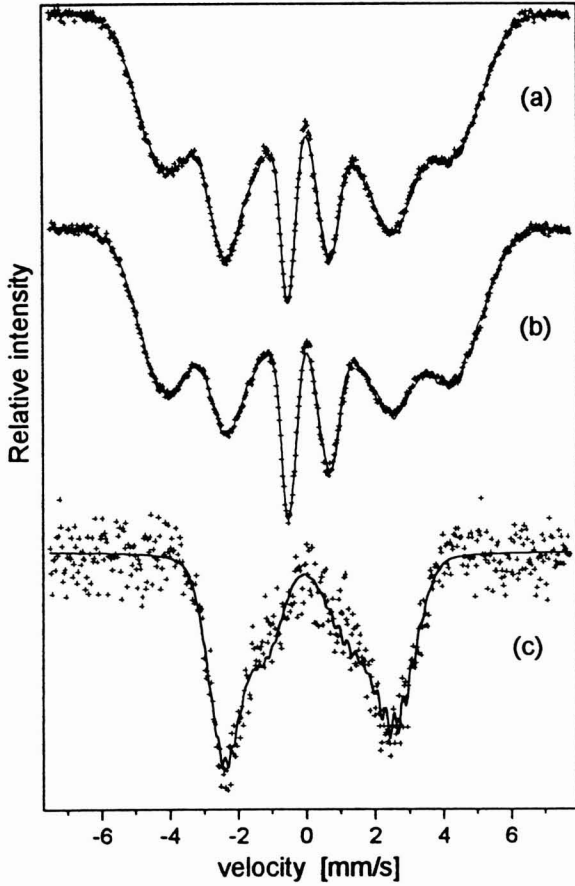


Fig. 16 Mössbauer spectra of amorphous $\text{Fe}_{93}\text{Zr}_7$ measured at 4.2 K (a) and in 1 T perpendicular applied field (b). Linear combination of these two spectra gives the separated 2-5 lines (c).

oriented antiparallel to the magnetic moment, i.e. to the applied field. It means that above saturation (i.e. in the collinear state) the absolute value of the hyperfine field should decrease in direct proportion to the applied field. (In the following B_{hf} marks the absolute value of the Fe hyperfine field, its average value is $\langle B_{\text{hf}} \rangle$). The absolute value of the average effective hyperfine field at the ^{57}Fe nucleus is given approximately by

$$\langle B_{\text{hf}} \rangle = \langle B_{\text{hf}}(B_{\text{ext}}=0) \rangle - B_{\text{ext}} + B_{\text{demag}},$$

where B_{demag} is the value of the demagnetization field.

When the applied field is compensated for, i.e. the quantity defined as $B_{\text{plus}} = \langle B_{\text{hf}} \rangle + B_{\text{ext}}$ is plotted vs B_{ext} , a saturation with zero slope is expected above the demagnetization field in the ferromagnetic state if no induced moment is present. The saturation value should be $\langle B_{\text{hf}}(B_{\text{ext}}=0) \rangle + B_{\text{demag}}$, i.e. the value of the hyperfine field extrapolated to $B_{\text{ext}}=0$ should differ from that of measured without external field by the value of the demagnetization field.

The ferromagnetic $\text{Fe}_{88}\text{Zr}_{12}$ approaches this behaviour as shown in Fig. 17. The deduced value of B_{demag} is about 1.3 T in good agreement both, with the value obtained from the $I_{2,5} \rightarrow 0$ extrapolation and with that of calculated from $4\pi M$. The case of $\text{Fe}_{93}\text{Zr}_7$ is also shown in Fig. 17. In

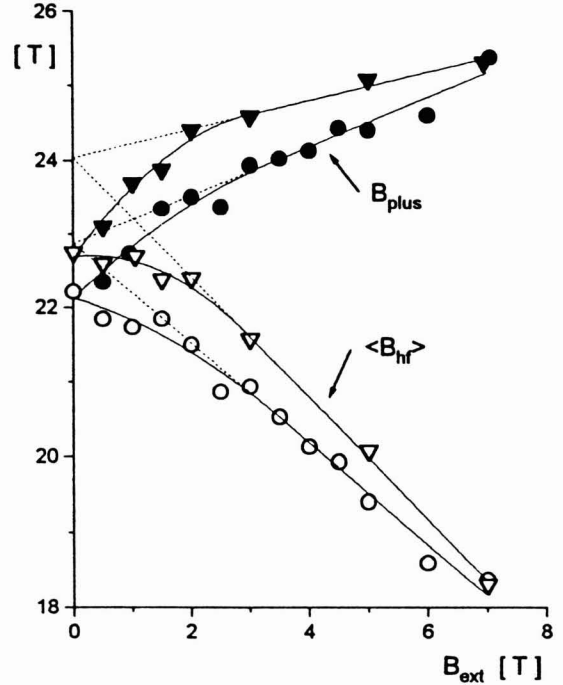


Fig. 17 External field dependence of the average hyperfine field $\langle B_{\text{hf}} \rangle$ (empty symbols) and $B_{\text{plus}} = \langle B_{\text{hf}} \rangle + B_{\text{ext}}$ (full symbols) at 4.2 K for amorphous $\text{Fe}_{88}\text{Zr}_{12}$ (triangles) and $\text{Fe}_{93}\text{Zr}_7$ (circles), respectively. The full lines are guides to the eye, the broken lines are linear extrapolations.

contrast to the expected saturation a significant induced moment is observed: the increase in B_{comp} cannot be explained with the demagnetization field.

The slope of B_{plus} vs B_{ext} determines the magnitude of the induced hyperfine field, i.e. the value of the induced Fe magnetic moment. Figure 18 shows the composition dependence of the bulk and the local susceptibilities in relative units. For the local susceptibility, $\Delta B_{\text{plus}} / (B_{\text{plus}} \Delta B_{\text{ext}})$ is plotted (where $\Delta B_{\text{plus}} = B_{\text{plus}}(B_{\text{ext}}=7\text{T}) - B_{\text{plus}}(B_{\text{ext}}=5\text{T})$, $B_{\text{plus}} = 1/2 [B_{\text{plus}}(B_{\text{ext}}=7\text{T}) + B_{\text{plus}}(B_{\text{ext}}=5\text{T})]$, $\Delta B_{\text{ext}} = 2\text{T}$), which is a direct (model independent) experimental measure of the Fe high field susceptibility between 5 T and 7 T normalized to the Fe magnetic moment. This combination eliminates the need to use the proportionality constant between hyperfine field and magnetic moment and substantially reduces the effect of any possible systematical errors in the evaluation of $\langle B_{\text{hf}} \rangle$. Moreover, the difference between $B_{\text{ext}}=5\text{T}$ and 7 T was chosen because most of the alloys was found to be collinear already in 5 T.

The composition dependence of this local Fe susceptibility is in good agreement with the similarly normalized high field bulk magnetization values, $\Delta M / (M \Delta B_{\text{ext}}) = \chi_{\text{hf}} / M$ as seen in Fig. 18. (In Ref. [57] only model dependent χ_{hf} values were given, so the presented values were calculated from the data in Fig. 1 of Ref. [57]). Data are also shown for amorphous $\text{Fe}_{70}\text{Ni}_{20}\text{Zr}_{10}$ where the field dependence is much weaker.

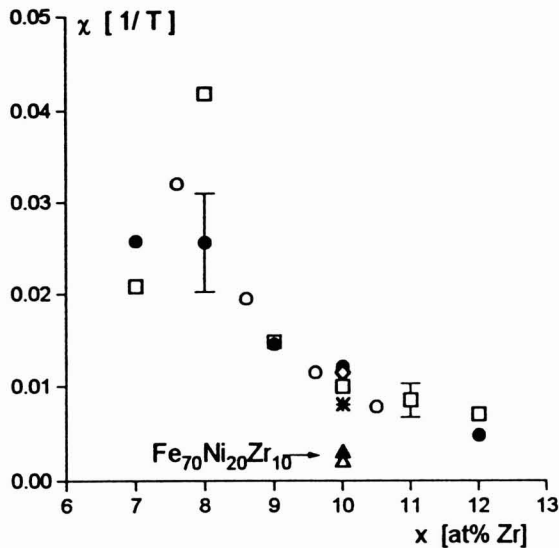


Fig. 18 Composition dependence of the normalized high field susceptibility $\chi_{hf} = \Delta Y / (Y \Delta B_{ext})$ between 5T and 7T. The full circles corresponding to the local Fe susceptibility are the present Mössbauer results, where Y stands for the compensated hyperfine field $B_{plus} = \langle B_{hf} \rangle + B_{ext}$. The corresponding quantity taken from literature bulk magnetization data ($Y=M$) are also shown: squares [2], circles [57], rhomb [58], and star [59]. The Mössbauer and magnetization [59] results (solid and empty triangles, respectively) are given for amorphous $Fe_{70}Ni_{20}Zr_{10}$ too. Typical error bars are marked.

The good agreement between the high field susceptibilities obtained from magnetization measurements and iron hyperfine field data is not unexpected since the analysis of $I_{2,5}$ has already shown the collinearity of the magnetic moments in these alloys. Moreover it excludes a possible spin-flip of a small percentage of antiferromagnetically aligned moments. In this case χ_{hf} obtained in the magnetization measurements were much larger than the χ_{hf} deduced from the hyperfine fields, since the hyperfine field reflects the absolute value of the iron magnetic moments.

IV. SUMMARY

The present Mössbauer spectroscopy and magnetic investigations of the composition, temperature and field dependence of the amorphous Fe-Zr alloys confirm that the magnetic properties of iron atoms depend strongly on the local environment in this system. Two main groups of iron atoms were distinguished. One group is identified with iron atoms surrounded exclusively with iron: their average magnetic moment is about $1 \mu_B$ and their atomic volume is somewhat smaller than the average iron volume as indicated by the isomer shift data. The other group is formed by the rest of the iron atoms: they have at least one Zr nearest neighbours and their average magnetic moment is about $1.8 \mu_B$. Broad distribution of magnetic moments is found around these average values. The observed atomic volume dependence of the iron magnetic moment follows the trend established in theoretical calculations. The relative number of the two kind of iron atoms is well approximated by the random statistical distribution of Zr atoms: no sign of

significant amount of chemical clustering was observed.

The magnetic coupling of these two sites to their surroundings differ considerably as deduced from the temperature dependence of the magnetic moment (i.e. hyperfine field) distributions. The iron sites with Zr nearest neighbours are coupled ferromagnetically to each other while the low moment of the iron atoms with iron nearest neighbours only are essentially decoupled from the moments of its surrounding. The existence of the decoupling is attributed to the well-known anomalous volume dependence of the magnetic properties of iron. Recent theoretical calculation of exchange interactions in amorphous Fe [7] allows the possibility of weak coupling between very close atoms. Even if we keep in mind the severe limitations of the model used in the present work to deduce these conclusions (molecular field model, second order perturbation series, nearest neighbour interaction approach) the observed temperature dependences can not be easily reconciled with the presence of a substantial antiferromagnetic exchange interaction.

The Mössbauer studies performed in large applied fields further elucidate this description. Indirect argument against the presence of a considerable amount of frustrated exchange interaction is the observation that the magnetic structure is already collinear in magnetic fields which are much lower than the values expected on the base of interaction strengths characteristic of the freezing temperature. The collinear state is reached in laboratory-scale magnetic fields, which suggest the existence of significant size collinear regions even before the application of the external field. In the field induced collinear magnetic state the value of the extremely large high field susceptibility is the same for the matrix, measured by bulk magnetization measurement and locally for the individual Fe magnetic moments measured via the hyperfine field, thus directly supporting the absence of antiferromagnetically aligned Fe moments.

On the other hand, the field dependent Mössbauer measurements confirm the spin freezing phenomena in these alloys posing the delicate question of its origin in a system without the hint of exchange frustration or strong magnetic anisotropy. The proposed decoupling of the moment of iron atoms with only iron nearest neighbours might be the cause of the observed freezing. In this bond percolation problem the number of iron atoms surrounded exclusively with iron is increasing with increasing iron concentration, resulting in magnetically separated regions. Thus magnetic clustering will occur on purely statistical basis unrelated to any hypothetical chemical clustering. The spin glass state is achieved when the percolation threshold is reached, i.e. the infinite ferromagnetic cluster cease to exist. Computer simulation shows [60] that the shape of the irregular separated regions deviates significantly from a spherical shape. The freezing of the direction of the collinear regions thus will be caused by the shape anisotropy of these percolation clusters. Characteristic feature of the shape anisotropy is that the direction of the magnetization and the applied field will only coincide in rather special circumstances which is not fulfilled for these percolation

clusters with fractal structure. This kind of shape anisotropy may explain the characteristic contradictory magnetic properties of spin glasses: fast increase of the magnetization in low fields, slow approach to saturation in high applied fields. The situation is further complicated in the Fe-Zr system, where the external magnetic field induces a significant surplus magnetic moment. The questions, whether this induced moment is of dynamic origin and whether it is a general feature of the spin glass behaviour are the actual open questions for further research.

ACKNOWLEDGEMENT

This work was supported by the Hungarian National Research Fund OTKA-T4464 and T17456.

REFERENCES

- [1] See, for a review, K. Fukamichi, T. Goto, H. Komatsu, and H. Wakabayashi, in *Proceedings of Fourth International Conference on the Physics of Magnetic Materials, Warsaw, 1988*, edited by W. Gorzkowski, K. Lachowicz, and H. Szymczak (World Scientific, Singapore, 1989), p. 354.
- [2] D.H. Ryan, J.M.D. Coey, E. Batalla, Z. Altounian, and J.O. Ström-Olsen, *Phys. Rev. B* **35**, 8630 (1987).
- [3] T. Kemény, F.J. Litterst, I. Vincze and R. Wäppling, *J. Phys. F* **13**, L37 (1983).
- [4] Y. Kakehashi, *Phys. Rev. B* **41**, 9207 (1990); **43**, 10820 (1991).
- [5] S. Krompiewski, U. Krey, U. Krauss, and H. Ostermeier, *J. Magn. Magn. Mat.* **73**, 5 (1988); U. Krey, S. Krompiewski, and U. Krauss, *ibid.* **86**, 85 (1990); U. Krauss and U. Krey, *ibid.* **98**, L1 (1991); U. Krey, U. Krauss, and S. Krompiewski, *ibid.* **103**, 37 (1992).
- [6] Y.N. Xu, Y.H. He, and W.Y. Ching, *J. Appl. Phys.* **69**, 5460 (1991).
- [7] R.F. Sabiryanov, S.K. Bose, and O.N. Mryasov, *Phys. Rev. B* **51**, 8958 (1995).
- [8] I. Turek, Ch. Becker and J. Hafner, *J. Phys. Cond. Matter*, **4**, 7257 (1992); J. Hafner, M. Tegze and Ch. Becker, *Phys. Rev. B* **49**, 285 (1995); R. Lorenz and J. Hafner, *J. Magn. Magn. Mater.* **139**, 209, (1995).
- [9] H. Hiroyoshi and K. Fukamichi, *Phys. Lett. A* **85**, 242 (1981); *idem*, *J. Appl. Phys.* **53**, 2226 (1982).
- [10] S.N. Kaul, *J. Phys. F* **18**, 2089 (1988); R. Reisser, M. Fahnle and H. Kronmüller *J. Magn. Magn. Mat.* **75**, 45 (1988).
- [11] H. Yamauchi, H. Onodera, and H. Yamamoto, *J. Phys. Soc. Japan* **53**, 747 (1984); K. Wünsch and M. Rosenberg, *J. Appl. Phys.* **61**, 4401 (1987).
- [12] R. Reisser, M. Seeger, M. Fahnle and H. Kronmüller, *J. Magn. Magn. Mater.* **110**, 32 (1992).
- [13] S. N. Kaul and P. D. Babu, *Phys. Rev. B* **45**, 295 (1992).
- [14] S.N. Kaul, *J. Appl. Phys.* **61**, 451 (1987).
- [15] N. Saito, H. Hiroyoshi, K. Fukamichi, and Y. Nakagawa, *J. Phys. F* **16**, 911 (1986).
- [16] G. K. Nicolaidis and K. V. Rao, *J. Magn. Magn. Mater.* **125**, 195 (1993).
- [17] S. Hadjoudj, S. Senoussi, and D.H. Ryan, *J. Appl. Phys.* **67**, 5958 (1990); S. Hadjoudj, S. Senoussi, and I. Mirebeau, *J. Magn. Magn. Mat.* **93**, 136 (1991).
- [18] J.J. Rhyne, R.W. Erwin, J.A. Fernandez-Baca and G.E. Fish, *J. Appl. Phys.* **63**, 4080 (1988); J.A. Fernandez-Baca, J.J. Rhyne, R.W. Erwin and G.E. Fish, *J. de Physique* **49**, C8-1207 (1988).
- [19] K. Mergia, S. Messoloras, G. Nicolaidis, D. Niarchos and R. J. Stewart, *J. Appl. Phys.* **76**, 6380 (1994).
- [20] M. Ghafari, N. Chmielek, W. Keune, and C.P. Foley, *Hyperfine Interact.* **54**, 527 (1990).
- [21] D.H. Ryan, J.O. Strom-Olsen, R. Provencher and M. Townsend, *J. Appl. Phys.* **64**, 5787 (1988).
- [22] D.A. Read, T. Moyo, and G.C. Hallam, *J. Magn. Magn. Mat.* **44**, 279 (1984); D.A. Read, T. Moyo, S. Jassim, R.A. Dunlop and G.C. Hallam, *J. Magn. Magn. Mat.* **82**, 87 (1989).
- [23] H. Kronmüller, V.A. Ignatchenko and A. Forkl, *J. Magn. Magn. Mater.* **134**, 68 (1994).
- [24] T. Dumelow, P.C. Riedi, P. Mohn, K. Schwarz and Y. Yamada, *J. Magn. Magn. Mat.* **54-57**, 1081 (1986).
- [25] M. Ghafari, U. Gonser, H.-G. Wagner and M. Naka Nucl. Inst. Meth. **199**, 197 (1982).
- [26] D. Kaptás, T. Kemény, L. F. Kiss, L. Gránásy, J. Balogh and I. Vincze, *J. Non-Cryst. Solids* **156-158**, 336 (1993).
- [27] I. Vincze, D. Kaptás, T. Kemény, L.F. Kiss and J. Balogh, *Phys. Rev. Letters*, **73**, 496 (1994).
- [28] I. Vincze, *Solid St. Commun.* **25**, 689 (1978); *Nucl. Inst. Meth.* **199**, 247 (1982).
- [29] H. Ma, H.P. Kunkel and G. Williams, *J. Phys. Condens. Matter*, **3**, 5563 (1991).
- [30] H. Yamamoto, H. Onodera, K. Hosoyama, T. Masumoto, and K. Yamauchi, *J. Magn. Magn. Mat.* **31-34**, 1579 (1983).
- [31] H. Kobayashi, H. Onodera and H. Yamamoto, *J. Phys. Soc. Japan* **55**, 331 (1986).
- [32] M. Ghafari, W. Keune, R.A. Brand, R.K. Day, and J.B. Dunlop, *Mat. Sci. Eng.* **99**, 65 (1988).
- [33] M. Ghafari, N. Chmielek, W. Keune and C.P. Foley, *Physica B* **161**, 222 (1989).
- [34] D. Kaptás and I. Vincze, *Hyperfine Interact.* **55**, 987 (1990).
- [35] D.H. Ryan and H. Ren, *J. Appl. Phys.* **69**, 5057 (1991).
- [36] H.S. Chen, K.T. Aust, and Y. Waseda, *J. Non-Cryst. Solids* **46**, 307 (1981).
- [37] Y. Waseda, T. Masumoto, and S. Tamaki, *Proc. Conf. on Metallic Glasses: Science and Technology, Budapest 1980*, Editors: C. Hargitai, I. Bakonyi, and T. Kemény, Vol. 1, p. 369.
- [38] M. Laridjani, J.F. Sadoc, and P. Leboucher, *Z. Phys. Chem.* **157**, 17 (1988); M. Laridjani and J.F. Sadoc, *Int. J. Mod. Phys. B* **2**, 37 (1988).
- [39] H. Maeda, H. Terauchi, N. Kamijo, M. Hida and K. Osamura, *Proc. 4th. Int. Conf. on Rapidly Quenched Metals, Sendai, 1981*, p. 397.
- [40] P. Kizler, P. Lamparter and S. Steeb, *Z. Naturforsch.* **44a**, 7 (1989); P. Kizler, *Phys. Rev. B* **48**, 12488 (1993).
- [41] K.M. Unruh and C.L. Chien, *Phys. Rev. B* **30**, 4968 (1984).
- [42] D.A. Williamson, in *Mössbauer Isomer Shifts*, eds. G.K. Shenoy and F.E. Wagner, North-Holland, Amsterdam, 1978, p. 337.
- [43] H. Ren and D.H. Ryan, *Phys. Rev. B* **51**, 15885 (1995).
- [44] H. Keller, *J. Appl. Phys.* **52**, 5268 (1981).
- [45] B. Window, *J. Phys. E: Sci. Instrum.* **4**, 401 (1971).
- [46] H. Lerchner and M. Rosenberg, *Hyperfine Interact.* **19**, 51 (1988).
- [47] S. N. Kaul, V. Siruguri and G. Chandra, *Phys. Rev. B* **45**, 12343 (1992).
- [48] D. Kaptás, T. Kemény, L.F. Kiss, J. Balogh, L. Gránásy and I. Vincze, *Phys. Rev. B* **46**, 6600 (1992).
- [49] H. Ren and D.H. Ryan, *J. Appl. Phys.* **70**, 5837 (1991).
- [50] B. Huck and J. Hesse, *J. Magn. Mat. Mat.* **78**, 247 (1989).
- [51] P.L. Paulose, V. Nagarajan and R. Nagarajan, *Hyperfine Interact.* **34**, 477 (1987).

- [52] M. Ghafari, W. Keune, N. Chmielek, R.A. Brand, M.F. Braun and M. Maurer, *J. de Physique* **49**, C8-1145 (1988).
- [53] S.N. Kaul, C. Bansal, T. Kumeran, and M. Havalgi, *Phys. Rev.* **B38**, 9248 (1988).
- [54] J. Lauer and W. Keune, *Phys. Rev. Lett.* **48**, 1850 (1982); I.A. Campbell, S. Senoussi, F. Varret, J. Teillet and A. Hamzic, *Phys. Rev. Lett.* **50**, 1615 (1983); R.A. Brand, H. Georges, J. Hubsch and J.A. Heller, *J. Phys. F*, **15**, 1987 (1985).
- [55] I. Vincze, D. Kaptás, T. Kemény, L.F. Kiss, and J. Balogh, *J. Magn. Magn. Mat.* **140-144**, 297 (1995).
- [56] I. Vincze, J. Balogh, Z. Fóris, D. Kaptás and T. Kemény, *Solid St. Commun.* **77**, 757 (1991).
- [57] H. Hiroyoshi and K. Fukamichi, in *High Field Magnetism*, ed. M. Date (North-Holland, Amsterdam, 1983), p. 113.
- [58] S.N. Kaul, *Phys. Rev.* **B27**, 6923 (1983).
- [59] Shen Bao-gen, Xu Rufeng, Zhao Jian-gao, and Zhan Wen-shan, *Phys. Rev.* **B43**, 11005 (1991).
- [60] F. Family, T. Vicsek, and P. Meakin, *Phys. Rev. Letters* **55**, 641 (1985).